6.5 CLIMATE CHANGE PROJECTIONS IN THE UPPER DANUBE (EUROPEAN ALPS) AND THE UPPER BRAHMAPUTRA (HIMALAYAS)

Bodo Ahrens* and Andreas Dobler
IAU, Goethe-University, Frankfurt am Main, Germany

1 INTRODUCTION

Coarse-grid global circulation models (GCMs) do not allow for regional estimates of water balance or trends of extreme precipitation. This is especially true in complex terrain. Therefore, downscaling of the global simulations to generate regional precipitation is necessary. This paper discusses dynamical and statistical downscaling in two major river basins (RBs): (1) the upper Danube river basin (UDRB) covering an area of 76'653 km^2 in the European Alps and (2) the upper Brahmaputra river basin (UBRB) with about 500'000 km^2 in the Himalayas. The discussion focuses on simulated changes of daily precipitation statistics in the two RBs.

2 METHODS

A detailed evaluation of dynamical and statistical downscaling methods applied to ERA40 (Uppala et al., 2003) re-analysis data in both regions is given in Dobler and Ahrens (2008). In the present study, large-scale projections using the IPCC SRES A1B emission scenario are downscaled.

The large-scale projections are generated with the ECHAM5 model (Roeckner et al., 2006) and have a grid resolution of about 2°. For dynamical downscaling the regional climate model CLM is used with a grid resolution of 0.44°. As a parsimonious statistical downscaling method we use a method based on mapping daily precipitation to a two-parameter gamma distribution (for further details see Dobler and Ahrens, 2008). In the following sections, statistically downscaled ECHAM5 precipitation fields are named ECHAM5-Γ. They have a grid resolution of 0.5°.

Trends of daily precipitation statistics are calculated for all four seasons of the years during the simulation period 1960-2080. An overview on the precipitation statistics is provided in Table 1. The wet day threshold is set to be 1 mm/d. Beside the two major RBs, 5 sub-areas of interest (see Figs. 1 and 2) are considered. The sizes of the single areas (in number of grid points on the 0.44° simulation grids) are: UDRB 51, Lech RB 5, Salzach RB 7, UBRB 275, Assam 47, Lhasa RB 22 and Wang-Chu RB 8. For the very small Wang-Chu, Lech, and Salzach RBs, a bounding box of 4 x 4 grid points has been used to evaluate the trends in the climate projections.

Table 1: List of precipitation statistics.

Acronym	Description	Unit
PFRE	Fraction of wet days	1
PINT	Mean precipitation amount on wet days	mm/d
PQ90	90% quantile of wet days precipitation	mm/d
PX5D	Max. 5-day precipitation	mm
PCDD	Longest period of consecutive dry days	d

2.1 Evaluation

Figures 3 and 4 show precipitation climates from different observation data sets, the ERA40 re-analysis data, the CLM, the ECHAM5, and the ECHAM5-Γ precipitation in the UDRB and

* *Corresponding author address:* Bodo Ahrens, Institute for Atmospheric and Environmental Sciences, Goethe-University, Altenhöferallee 1, 60438 Frankfurt am Main, Germany. e-mail: bodo.ahrens@iau.uni-frankfurt.de

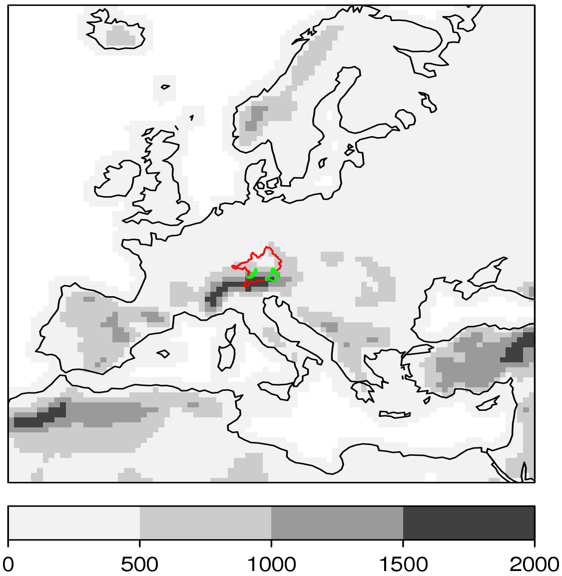

Figure 1: Orography (m) used for the regional climate simulations with the CLM. The colored areas denote the Upper Danube (red), the Lech (left), and the Salzach (right) river basins.

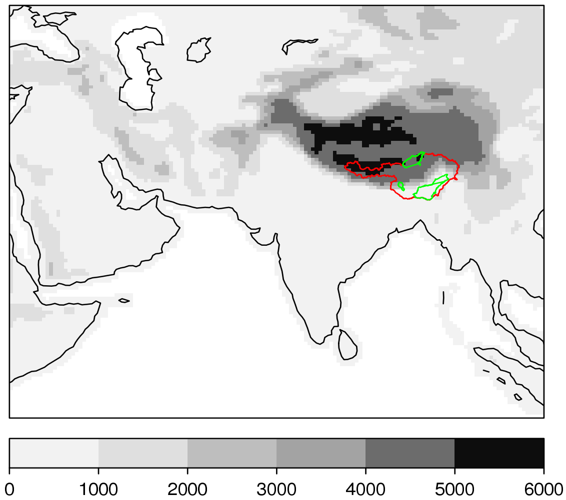

Figure 2: As for Fig. 1, but for the South Asian computational domain with the Assam region (bottom right) and the Upper Brahmaputra (red), the Lhasa (top) and the Wang-Chu (bottom left) river basins.

the UBRB, respectively. The observation data sets shown are GPCC (Schneider et al., 2008), UDEL (Legates et al., 1990) and CRU (Mitchell and Jones, 2005) in both RBs as well as the Frei-Schär data set version 4.1 (Frei and Schär, 1998) in the UDRB and the East Asia Daily Precipitation data set (Xie et al., 2007) in the UBRB.

The main deficiencies of the CLM are apparent in the UBRB during the monsoon season, when it underestimates the observed precipitation. This is consistent with the findings of Rockel and Geyer (2008), that the CLM highly underestimates the monthly precipitation in this region from June to August. This finding is not surprising because the model was not designed for this climate region. Nevertheless, the accuracy of CLM precipitation at the 0.5° scale is comparable with that of ERA40 precipitation, and in most places even comparable with that of statistically downscaled ERA40 precipitation (see Dobler and Ahrens, 2008).

As was already shown by Hagemann et al. (2005), the ERA40 precipitation strongly overestimates precipitation in the Ganges-Brahmaputra region. Despite the deficiencies of the CLM during the monsoon season, it yields much better results than the large-scale ERA40 and ECHAM5 precipitation in this region. The best results in this region however, are obtained

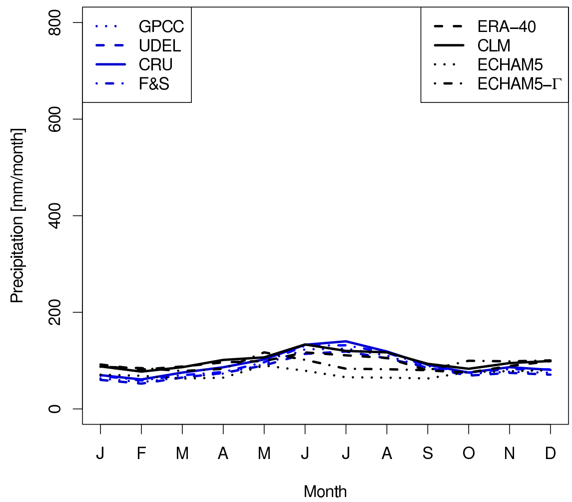

Figure 3: Precipitation climates from different observation data sets (blue), the ERA40 re-analysis and model simulations in the UDRB for the time period 1971-1999.

by the ECHAM5-Γ precipitation.

Still, the CLM is a promising method for downscaling of GCM projections. Moreover, the CLM has an advantage over the statistical method, in that it yields a consistent set of different meteorological parameters that can be used, for example, as input to a hydrological model.

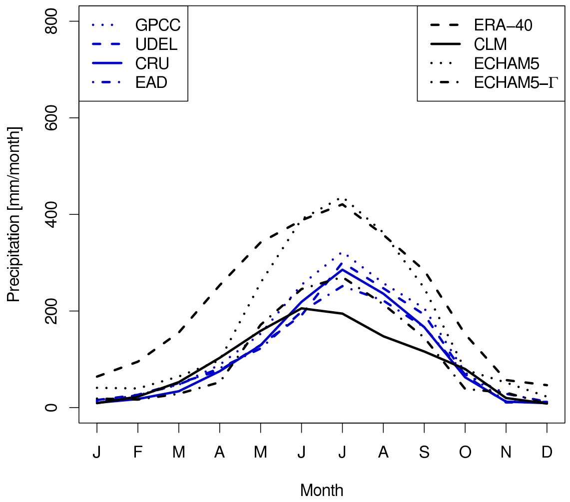

Figure 4: As for Fig. 3, but for the UBRB and the time period 1978-2000.

2.2 Model bias correction

Regional and global climate models commonly show model biases in, for example, rain day frequency and rain day intensity. However, to assess the question of a changing climate, projections from these models are usually normalized with respect to some reference period (in this study: 1971-2000). Via this normalization (i.e., division by the mean value of the reference period), constant model biases are removed from the model results.

A more complex bias correction is performed, when applying the statistical downscaling method to the coarse-grid precipitation. But, comparing the ECHAM5-Γ precipitation to normalized ECHAM5 precipitation we have found only small differences in the changes of the statistical values (not shown). The same statistical method can also be used to remove model biases from the CLM model. There too, the changes of the statistical values are very similar in the raw and the bias corrected CLM precipitation fields (not shown).

We conclude that, for the calculation of changes in precipitation statistics as simulated by the ECHAM5 or the CLM model, a simple normalization is sufficient to remove most of the model biases. There is only a small added value from the more complex methods. This is however only true, as long as the model is at the end of the simulation chain and no additional model (e.g., a hydrological model) is driven by the precipitation fields.

3 RESULTS

Figures 5 and 6 show the normalized annual and seasonal precipitation totals in the UDRB and the UBRB as modelled by the CLM. For the European regions the seasons are spring (MAM), summer (JJA), autumn (SON) and winter (DJF). For the South Asian regions these are summer (MAM), monsoon (JJAS), post-monsoon (ON) and winter (DJF) as suggested by Basistha et al. (2008).

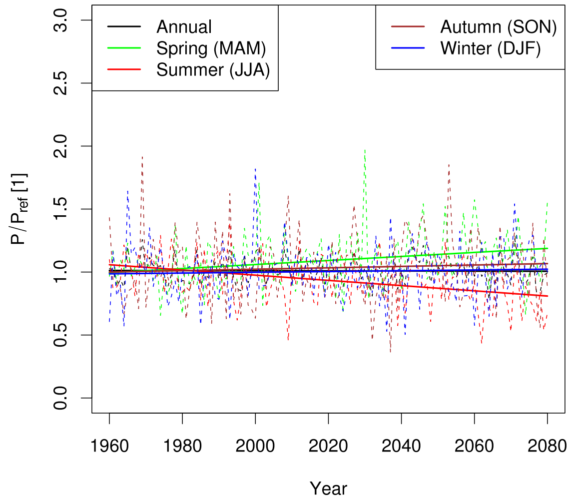

Figure 5: Annual and seasonal precipitation changes in the UDRB. Dotted lines denote CLM projections, solid lines linear fits. The CLM projections have been normalized using the reference period 1971-2000.

Annual precipitation shows no trends in either the UDRB or the UBRB. In the UDRB, there are positive trends in spring, autumn and winter, and a negative trend in summer. However, only the positive trend in spring and the negative trend in summer are significant (at the 0.05 level, see also Table 2). In the UBRB there are positive trends in summer and the post-monsoon season, and negative trends in the monsoon season and in winter. Here, all trends, except the positive trend in the post-monsoon season are significant.

Table 2 gives the precipitation trends in the UBRB, the UDRB and the sub-areas during the time period 1960-2080. The table shows the values for the annual as well as seasonal precipitation sums as simulated by the CLM and the ECHAM5 model. Only values in bold are statistically significant.

In the UDRB and the sub-areas, the ECHAM5

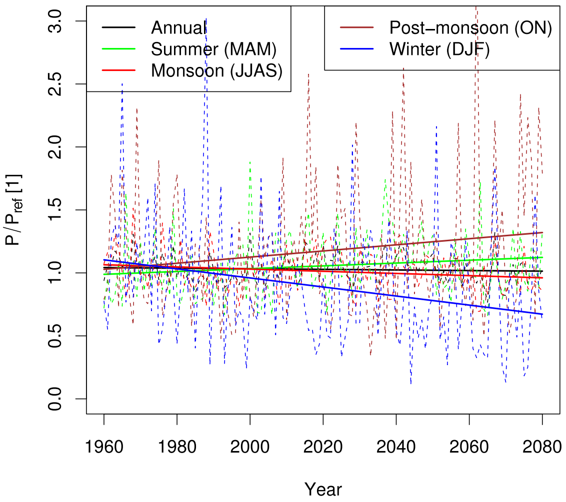

Figure 6: As for Fig. 5, but for the UBRB.

Table 2: Annual and seasonal precipitation changes (% / 100 years) in different areas during the time period 1960-2080. The values are for A1B scenario projections from the CLM and the ECHAM5 model. For normalization, the yearly values have been divided by the mean of the reference period 1971-2000.

CLM	Ann.	MAM	JJA	SON	DJF
UDRB	-1	**16**	**-21**	6	3
Salzach	0	**19**	**-20**	7	0
Lech	-3	**15**	**-22**	2	0
ECHAM5					
UDRB	-2	6	**-27**	9	3
Salzach	-3	5	**-28**	13	0
Lech	-5	-2	**-29**	7	-1

CLM	Ann.	MAM	JJAS	ON	DJF
UBRB	-2	**11**	**-9**	24	**-36**
Wang-Chu	2	8	-2	34	**-45**
Assam	6	**23**	-11	120	2
Lhasa	**-11**	**-21**	-7	-6	**-46**
ECHAM5					
UBRB	-4	8	-6	-6	**-31**
Wang-Chu	**-9**	11	**-12**	-6	**-45**
Assam	2	**19**	-2	-1	-24
Lhasa	**-7**	-5	-7	-8	**-29**

model does not show the positive trend in spring precipitation shown by the CLM. Otherwise, there are no notable differences between the two models. In the Asian regions, the Lhasa RB shows a negative trend for annual precipitation in both models and a negative trend in summer precipitation in the CLM model. All regions except Assam show a negative trend in winter precipitation in both models. Overall, there are more disagreements between the two models than in the UDRB.

Table 3: As for Table 2, but for PFRE and seasonal values only.

CLM	MAM	JJA	SON	DJF
UDRB	5	**-24**	-3	-2
Salzach	6	**-21**	-4	-4
Lech	4	**-23**	-5	-3
ECHAM5				
UDRB	-3	**-25**	-8	-5
Salzach	-4	**-24**	-6	-9
Lech	-6	**-25**	-10	-7

CLM	MAM	JJAS	ON	DJF
UBRB	-5	**-15**	-7	**-42**
Wang-Chu	-1	**-14**	-5	**-45**
Assam	12	**-15**	29	-18
Lhasa	**-26**	**-17**	-17	**-48**
ECHAM5				
UBRB	-2	**-5**	-10	**-30**
Wang-Chu	4	**-2**	-13	-27
Assam	8	**-5**	-6	-15
Lhasa	-9	**-9**	**-18**	**-34**

Table 4: As for Table 3, but for PINT.

CLM	MAM	JJA	SON	DJF
UDRB	**11**	4	**10**	6
Salzach	**12**	1	**14**	**6**
Lech	**11**	1	**9**	3
ECHAM5				
UDRB	**9**	-5	**20**	**9**
Salzach	**10**	-8	**22**	**10**
Lech	5	-7	**19**	7

CLM	MAM	JJAS	ON	DJF
UBRB	**9**	**7**	33	0
Wang-Chu	4	**13**	42	-24
Assam	10	7	59	5
Lhasa	1	**11**	17	4
ECHAM5				
UBRB	6	-1	7	-10
Wang-Chu	5	**-10**	13	-35
Assam	11	3	5	-28
Lhasa	2	2	14	5

More daily precipitation statistics for the different seasons and areas are shown in Tables 3 to 6. There is a negative trend in PFRE in all areas and models in the second season of the year. For PINT, there are several positive trends in both models and regions. Note that for the Wang-Chu RB, the ECHAM5 simulations show a negative trend, where the CLM simulations show a positive trend. For PQ90 we found, that the trends agree to a large extend with the trends in PINT (not shown).

Table 5: As for Table 3, but for PX5D and the UDRB (top) and UBRB (bottom) only.

	MAM	JJA	SON	DJF
CLM	**17**	-3	3	-1
ECHAM5	**19**	**-17**	**17**	**8**

	MAM	JJAS	ON	DJF
CLM	10	6	38	-15
ECHAM5	11	**11**	11	-24

Table 6: As for Table 3, but for PCDD.

	MAM	JJA	SON	DJF
CLM	-3	**31**	-4	9
ECHAM5	1	**37**	7	21

	MAM	JJAS	ON	DJF
CLM	10	**21**	4	**21**
ECHAM5	5	**27**	16	**21**

For PX5D, the ECHAM5 model shows significant trends in all seasons in the UDRB, while the CLM shows only a positive trend in spring. The ECHAM5-Γ precipitation yields almost the same trends as the large-scale ECHAM5 precipitation (not shown). In the UBRB, there are no trends in the CLM projections and only a positive trend during the Monsoon season in the ECHAM5 projections. For PCDD there is high agreement between the two models in all seasons.

In Beniston et al. (2007), an increase by a factor of about 1.15 for the winter precipitation in the central European region was found for the CHRM model between the scenario period 2071-2100 and the control period 1961-1990. Using the daily precipitation data from the PRUDENCE project (see http://prudence.dmi.dk) we have calculated a factor of 1.11 for the UDRB.

Contrary, we see no significant trend in winter precipitation in the UDRB for the CLM and the ECHAM5 projections during the time period 1960-2080. However, if we look at scenario and control periods only, we also find a factor of 1.11 in the CLM projections. Here, as control period we have also used 1961-1990. But, because our current CLM simulation ends in the year 2080, we have used the years 2066-2080 as scenario period. Note that for the ECHAM5 projections, there is no notable difference between the scenario periods 2066-2080 and 2071-2100 and the factor we find is 1.1. The factors calculated for PFRE, PINT, and PQ90 are also in good agreement with the values shown in Beniston et al. (2007), both for summer and winter, CLM and ECHAM5 simulations.

4 CONCLUSIONS

Changes of daily precipitation statistics in the Upper Danube river basin (UDRB) and the Upper Brahmaputra river basin (UBRB) were calculated for global and regional climate model simulations for the time period 1960-2080. As expected, different scenarios evolve in the two river basins. For instance, there is a significant decrease in winter precipitation in the UBRB but no trend in the UDRB.

Between the two models, no big differences were found except for the maximum five day precipitation in the UDRB. A more detailed evaluation of this parameter should be kept in mind, as it is an indicator of extreme precipitation levels which may cause floodings. However, this evaluation is limited to some extend by the availability of daily precipitation data sets over long time periods.

Additionally, the global precipitaion projections were statistically downscaled. No noteable differences were found between the large-scale and the statistically downscaled precipitation fields in the trends of the considered precipitation statistics.

In this study, we focussed only on the SRES A1B scenario runs. A quick look showed, that the scenarios A2 and B1 show very similar results.

ACKNOWLEDGMENTS

This work was partly funded by the EC project BRAHMATWINN (Contract No. 036592

(GOCE)). Graphics were drawn and analyses performed using the open-source software package R (www.r-project.org). We also wish to acknowledge the COSMO consortium (cosmo-model.cscs.ch) and the CLM community (www.clm-community.eu) for access to and support in using the CLM model.

References

Dobler, A., B. Ahrens, 2008: Precipitation by a regional climate model and bias correction in Europe and South Asia. *Meteorol. Z.*, 17, in press.

Basistha, A., D. S. Arya, N. K. Goel, 2008: Analysis of historical changes in rainfall in the Indian Himalayas. *Int. J. Climatol.*, in press, DOI: 10.1002/joc.1706.

Beniston, M., D. B. Stephenson, O. B. Christensen, C. A. T. Ferro, C. Frei, S. Goyette, K. Halsnaes, T. Holt, K. Jylhä, B. Koffi, J. Palutikof, R. Schöll, T. Semmler, K. Woth, 2007: Future extreme events in European climate: An exploration of regional climate model projections, *Clim. Change*, 81, suppl. 1, 81 95.

Frei, C., C. Schär, 1998: A precipitation climatology of the Alps from high-resolution raingauge observations. *Int. J. Climatol.*, 18, 873-900.

Legates, D. R., C. J. Willmott, 1990: Mean Seasonal and Spatial Variability in Gauge-Corrected, Global Precipitation. *Int. J. Climatol.*, 10, 111-127.

Hagemann, S., K. Arpe, L. Bengtsson, 2005: Validation of the hydrological cycle in ERA-40. *ERA-40 project report series*, 24, ECMWF.

Mitchell, T.D., P.D. Jones, 2005: An improved method of constructing a database of monthly climate observations and associated high–resolution grids. *Int. J. Climatol.*, 25, 693-712.

Rockel, B., B. Geyer, 2008: Performance of the regional climate model CLM in different climate regions on the example of precipitation. *Meteorol. Z.*, 17, in press.

Roeckner, E., M. Lautenschlager, H. Schneider, 2006: IPCC-AR4 MPI-ECHAM5_T63L31 MPI-OM_GR1.5L40 SRESA1B run no.1: Atmosphere 6 HOUR values, *MPImet/MaD Germany*. World Data Center for Climate, DOI: 10.1594/WDCC/EH5-T63L31_OM-GR1.5L40_A1B_1_6H

Schneider, U., T. Fuchs, A. Meyer-Christoffer, B. Rudolf, 2008: Global Precipitation Analysis Products of the GPCC. Global Precipitation Climatology Centre (GPCC), DWD, Internet Publication, 1-12.

Uppala, S.M., P.W. Kallberg, A.J. Simmons, U. Andrae, V. da Costa Bechtold, M. Fiorino, J.K. Gibson, J. Haseler, A. Hernandez, G.A. Kelly, X. Li, K. Onogi, S. Saarinen, N. Sokka, R.P. Allan, E. Andersson, K. Arpe, M.A. Balmaseda, A.C.M. Beljaars, L. van de Berg, J. Bidlot, N. Bormann, S. Caires, F. Chevallier, A. Dethof, M. Dragosavac, M. Fisher, M. Fuentes, S. Hagemann, E. Holm, B.J. Hoskins, L. Isaksen, P.A.E.M. Janssen, R. Jenne, A.P. McNally, J–F. Mahfouf, J–J. Morcrette, N.A. Rayner, R.W. Saunders, P. Simon, A. Sterl, K.E. Trenberth, A. Untch, D. Vasiljevic, P. Viterbo, J. Woollen, 2005: The ERA-40 re-analysis. *Quart. J. Roy. Meteor. Soc.*, 131, 2961-3012.

Xie, P., A. Yatagai, M. Chen, T. Hayasaka, Y. Fukushima, C. Liu, S. Yang, 2007: A gauge-based analysis of daily precipitation over East Asia. *J. Hydrometeor.*, 8, 607-627.